# Optical and Electronic Simulation of Gallium Arsenide/Silicon Tandem Four Terminal Solar Cells

# Optical and Electronic Simulation of Gallium Arsenide/Silicon Tandem Four Terminal Solar Cells

*Vishnuvardhanan Vijayakumar and Dunbar P. Birnie, III*

Department of Materials Science & Engineering, Rutgers - State University of New Jersey, Piscataway, New Jersey 08854, USA.

Review Version – Final Paper Published as: Vishnu Vijayakumar and D. P. Birnie, III, "Optical and Electronic Simulation of Gallium Arsenide / Silicon Tandem Four Terminal Solar Cells", *Solar Energy*, **97**, 85-92, (2013) (DOI: 10.1016/j.solener.2013.07.033).

**Abstract**

A tandem solar cell in a mechanical (stack like) arrangement of gallium arsenide and silicon solar cells is evaluated as a pathway towards higher efficiency terrestrial solar cells. In this work the technical feasibility of the tandem solar cell is investigated. Here we report on the detailed electrical and optical simulations of this structure quantifying various theoretical and practical loss mechanisms in the interface and in the device and indicate that an efficiency improvement of 5.13% would be attainable with present generation of gallium arsenide and silicon solar cells in this configuration. The optical and electrical parameters for gallium arsenide and silicon simulation models were extracted from experimental devices and material vendors. The developed simulation models were validated by comparing the performance of standalone gallium arsenide and silicon solar cells with experimental devices reported in the literature.

**Keywords:** Tandem solar cell; Electronic Modeling; Optical modeling; Silicon solar cell;

## 1. Introduction:

Worldwide electricity consumption in 2008 was estimated to be 19.1 trillion KWh and it is projected to increase by 85% to reach 35.2 trillion KWh in 2035 according to US Energy Information Administration (2011). Though abundant fossil fuel reserves exist in the planet to support this growth in electricity consumption, concerns of global warming may limit its consumption. There is abundant solar energy irradiation on the planet to meet the worlds electricity demand and the cost of solar energy generation have also been falling rapidly bringing it closer to grid parity (Woodhouse et al., 2011). But the challenge has been intermittency of

solar energy sources and large land area required to generate the energy using present technologies. If 20% of the projected global electricity demand in 2035 is met by photovoltaic devices, contributing 7 trillion KWh, that would entail a global installation of 3.85 terra watts (TW) (considering average solar irradiation of 5000 Wh / sq.m per day). In 2011 about 70 GW of solar module manufacturing infrastructure was online (Mehta, 2012), so a couple of TW scale installation is possible in less than 20 years because of the decreasing solar costs and growing manufacturing capacity. However the corresponding land area required for 3.84 TW will be approximately 47000 sq. km with present generation of silicon solar cells having 16% ~ 18% efficiency. Such high land requirement would pose significant challenges for Asia, Western Europe and parts of Africa and South America, which are some of the most densely populated regions in the world.

A pathway to higher module efficiency at a reasonable cost increase is essential if solar energy is needed to play a significant part of the global electricity generation mix. Present generation of silicon solar cells have reached a laboratory efficiency of 24.7% (Zhao et al., 1999) and it has a theoretical efficiency of 33% as shown in figure 1. Higher power conversion efficiencies would be possible by efficient broadband absorption of solar spectrum (Henry, 1980). Various device architectures have been demonstrated for this purpose namely multi-junction (series-connected 2 terminal) solar cells (King et al., 2007, Bertness et al., 1990 and Karam et al., 1999) and mechanical tandem (stack like) solar cells (Burgess et al., 1988, Gee and Virshup, 1988, Gale et al., 1990, Liska et al., 2006, Flamand et al., 2009 and Ito et al., 2011). Mechanical tandem solar cell architecture is attractive because two separate devices could be developed independently targeting a specific part of the incident spectrum and subsequently put together to form a tandem module avoiding tunnel junctions. It is especially attractive if it can utilize the existing multi-giga watt manufacturing capacity of silicon solar cells. Figure 1 shows the theoretical power conversion efficiencies for two junction (mechanical stack) solar cells based on Shockley-Queisser's (Shockley and Queisser, 1961) calculations for AM 1.5 spectrum.

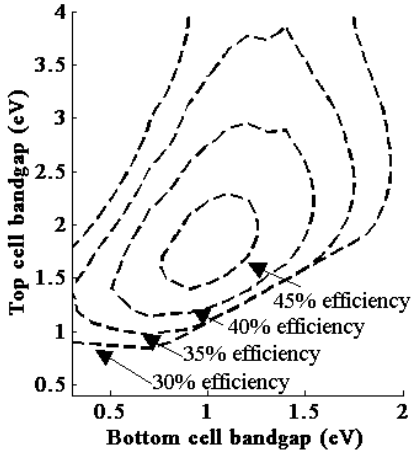


Fig. 1

In this work we examine a mechanical tandem structure with gallium arsenide as the high band gap top cell, which has a band gap of 1.43 eV, and silicon at 1.11 eV as the low band gap cell. The theoretical efficiency of a gallium arsenide / silicon tandem device is calculated to be as high as 44% as shown in figure 1. The increase in ideal theoretical efficiency compared to single junction silicon device is 11%, so a low cost, mass manufactured and efficient solar cell targeting high band gap spectrum in tandem with the silicon solar cell would be an attractive alternative for densely populated regions where land-area may limit installations. The illustration of the device architecture is shown in figure 2. We report here on the electrical and optical simulations of this tandem structure, quantifying the various theoretical and practical loss mechanisms in the encapsulation, interfaces and in the device. Based on these careful studies we find that a practical efficiency improvement of over 5% may be attainable in this configuration with present technology.

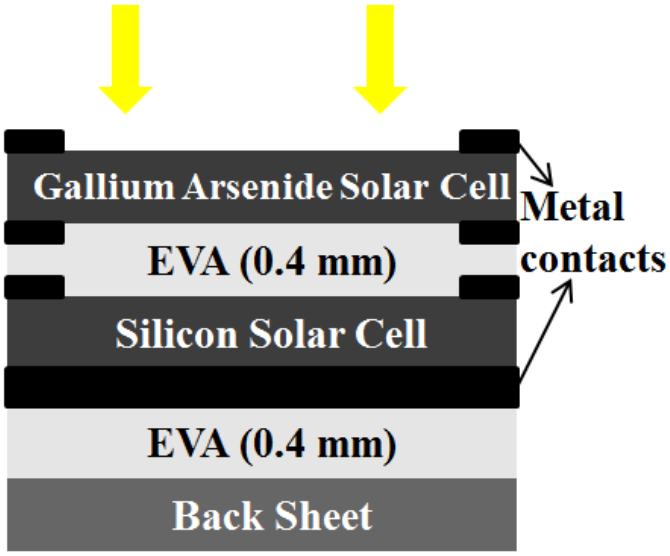


Fig.2 →

**Experimental - Device Modeling:**

The gallium arsenide solar cell was modeled as a thin film device with gallium indium phosphide window layer as shown in figure 3. Thin film gallium arsenide solar cell reduces the cost of the device by reusing the expensive gallium arsenide substrates. They have been demonstrated before (Bozler et al., 1981 and Bauhuis et al., 2009) and now Alta Devices Inc. (Mattos et al., 2011) is working to commercialize these devices. The device was modeled with a heavily doped n-type and p-type region at the front and back surface to form good ohmic contacts with the external metal contact (Belghachi and Helmaoui, 2008). A 0.025 μm thick gallium indium phosphide window layer is modeled to reduce the front surface recombination achieving a low rate of 200 cm/sec (Plá et al., 2007). Individual doping concentrations and thickness of the various gallium arsenide solar cell layers were based on the device fabricated and characterized by Lee et al (2011) with the emitter,

base and back surface field being 0.15 µm, 3.5 µm and 0.075 µm thick and the corresponding dopant concentrations being $1x10^{18}$, $2x10^{17}$ $4x10^{17}$ atoms/$cm^3$ respectively. The electron and hole mobilities, conduction band and valence band density of states and radiative recombination rate used in the simulation were obtained from Plá et al. (2007). Electron affinity and dielectric permittivity were obtained from Griggs et al. (2006). A two layer antireflection coating of magnesium fluoride and zinc sulfide is added in the simulation model on top of the gallium arsenide solar cell to reduce the reflection loss. The optical properties for magnesium fluoride and zinc sulfide coatings were obtained from experiments reported by Siqueiros et al. (1988). The thicknesses of the bi-layer antireflection coatings were optimized for the device by optical simulations through finite-difference time-domain method using Lumerical. The optical properties for the gallium arsenide solar cell were obtained from the optical constants handbook edited by Adachi (1999). The gallium arsenide solar cell device architecture that was simulated has metallic fingers as front and back contacts (Gee and Virshup, 1988 and Flamand et al., 2009) thereby allowing infrared light to pass through the device and be absorbed at the silicon solar cell below.

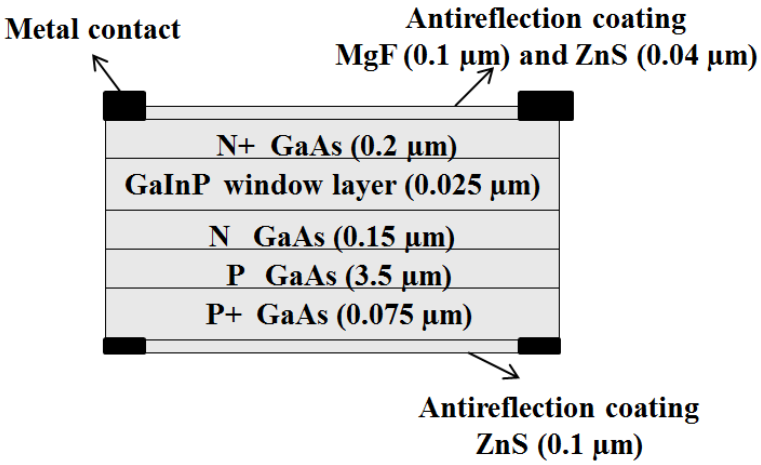


Fig. 3

The silicon solar cell device used in the simulation was modeled as a conventional silicon solar cell with p-type wafer. It was modeled with a heavily doped n-type and p-type region at the front and back surface to form good ohmic contacts with the external metal contacts (Lin and Chiou, 2012). Since SiNx which is used as an antireflection coating on silicon solar cells is also known to form good surface passivation at the emitter layer, the surface recombination rate for the front surface used in the simulation was 50 cm/sec as reported by Aberle (2000). At the back surface due to aluminum back surface field the surface recombination rate is low and it is approximately 250 ~ 300 cm/sec (Fellmeth et al., 2011). Illustration of the modeled silicon solar cells are shown in figure 4. Electron affinity, dielectric permittivity, conduction band and valence band density of states for silicon layer used in the simulation were based on the simulation parameters reported by Zhao et al., (2009) while electron and hole mobilities of silicon were obtained from the

simulation parameters reported by Dwivedi et al., (2013). Aluminum back surface field properties used in the simulation were based on the modeling and simulation experiments done by Dao et al., (2010). The emitter and base regions are 0.5 µm and 199.5 µm thick with a uniform dopant concentration of $10^{17}$ atoms/$cm^3$. The silicon solar cell was incorporated with mid gap and band tail defect states based on the values reported by Zhao et al., (2008). The optical properties for the silicon solar cell were obtained from the optical constants handbook edited by Adachi (1999).

Fig. 4 →

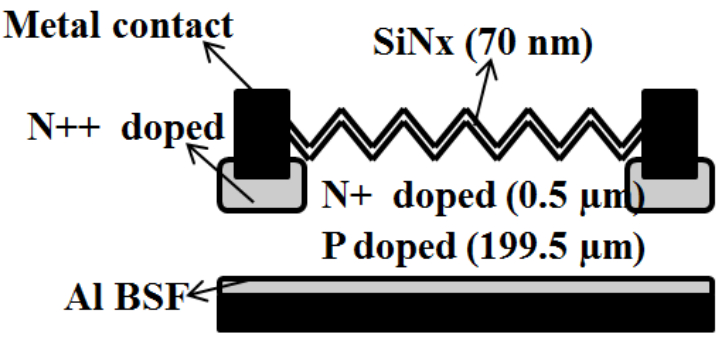


The electrical simulations of the modeled devices were performed using WxAMPS developed at University of Illinois (Liu et al., 2011). WxAMPS is a tool for numerical simulation of opto-electronic devices, an updated version of AMPS 1-D which is widely used for solar cell device simulations (Chen and Zhu, 2012). It allows for modeling of various recombination effects due to mid-gap states, Shockley-Read-Hall (S-R-H), band-band and incorporation of surface recombination effects. The simulation works by solving for Poisson's, electron and hole continuity equations iteratively. Optical modeling and simulation of the non-textured antireflective coated gallium arsenide device and the textured antireflective coated silicon device was done by finite-difference time-domain method using Lumerical. The thicknesses of the antireflective coatings were calculated through simulations, texturing of silicon solar cell was modeled based on the surface electron micrographs reported by Papet et al. (2006). Optical property data of SiNx antireflective layer was obtained from plasma enhanced chemical vapor deposition (PECVD) experiments Kang et al. (2011) and the optical property data of ethylene vinyl acetate (EVA) encapsulation layer was obtained from experiments performed by French et al. (2009). Figure 5 and figure 6 provide a plot of extinction coefficient and refractive index against wavelength of light for all the materials used in the simulation.

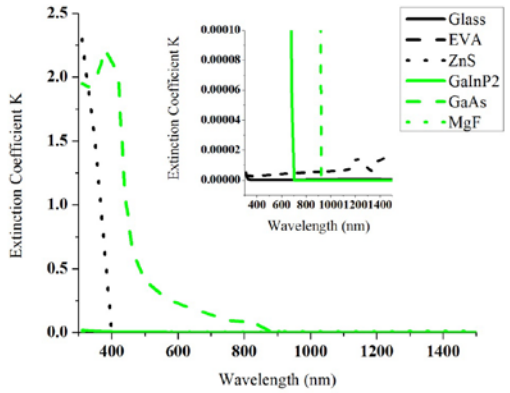


Fig. 5

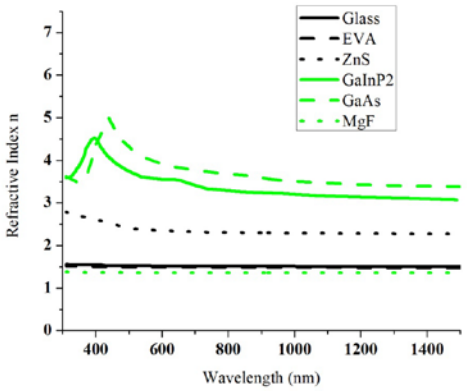


Fig. 6

## 3. Results & Discussion:

### 3.1. Optical losses in the top (Gallium Arsenide) solar cell:

Absorption and reflection losses at the magnesium fluoride and zinc sulfide anti-reflection coating layers for the gallium arsenide solar cell was calculated for AM 1.5 solar spectral intensity. The reflection loss at the air / MgF / ZnS / GaAs interface was on an average 2.6% for visible and infrared wavelengths up to 1117 nm i.e. the operating wavelengths of the tandem device, as shown in figure 7. Though reflection loss at UV wavelengths is high they correspond to a small part of the incident spectrum. Absorption loss due to zinc sulfide, shown in figure 7, is high at UV wavelengths because of the higher extinction coefficient near its absorption band edge which is at ~ 3.54 eV. However at visible and infrared wavelength regions absorption loss is very low, being on average around 0.2%. Also absorption loss of magnesium fluoride is less at 0.59% for the operational wavelengths of the tandem device as seen in figure 7. The total light intensity available at gallium arsenide layer is 881.5 watts / sq.m or ~88% of the total AM 1.5 spectral intensity, i.e. ~ 12% of the incident light energy is lost due to absorption and reflection losses. The light spectrum available at the silicon layer is shown in figure 8.

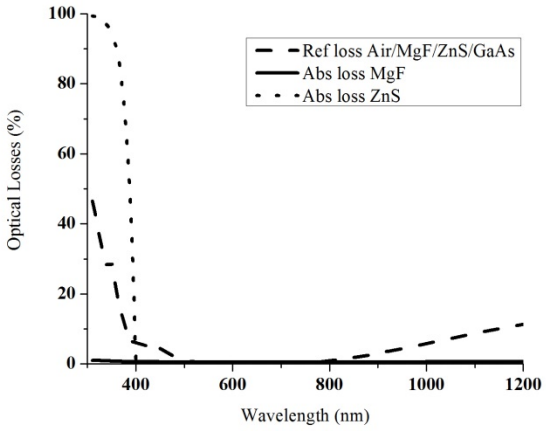


Fig. 7

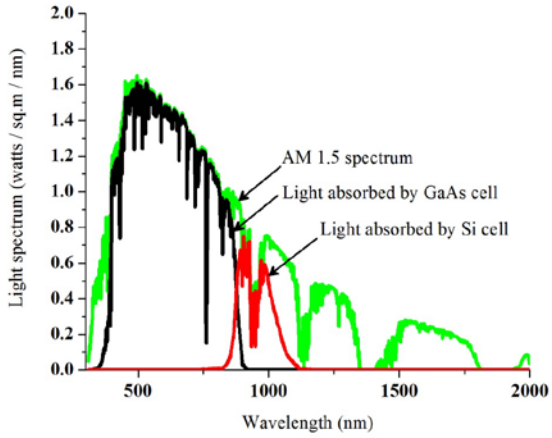


Fig. 8

### 3.2. Optical losses in the bottom (Silicon) solar cell:

As shown above in Figure 8, the longer wavelengths pass through the gallium arsenide device and reach the silicon device, a total of 281 W/m$^2$ or ~ 28% of the AM 1.5 spectral intensity. In order to optically couple the gallium arsenide and silicon solar cells, the bottom layer of gallium arsenide cell is modeled with an antireflective coating of zinc sulfide and the top layer of silicon cell is modeled with silicon nitride antireflective coating. A 0.2 mm layer of EVA, an encapsulant, is incorporated between the cells. The ZnS thickness was increased to reduce the reflection loss at longer wavelengths relevant for the silicon cell. Figure 9 shows the optical loss percentages at the various layers of the bottom solar cell before the light strikes the textured silicon layer. The SiNx antireflection coating thickness was optimized for reducing the reflection loss at the operation wavelengths of the bottom silicon solar cell therefore the reflection loss is higher for visible wavelengths as shown in figure 9. The reflection loss at GaAs/ZnS/EVA and EVA/SiNx/Si textured interfaces was on an average 0.3% and 1.54% respectively for operational wavelengths of the tandem silicon solar cell which is between 870 nm to 1200 nm. Absorption loss due to EVA, as shown in figure 9, is on average around 2.24% for operational wavelengths of the silicon solar cell. The total light intensity available at silicon layer is calculated to be 281 W/m$^2$ or ~ 28% of the total AM 1.5 spectral intensity.

Fig. 9

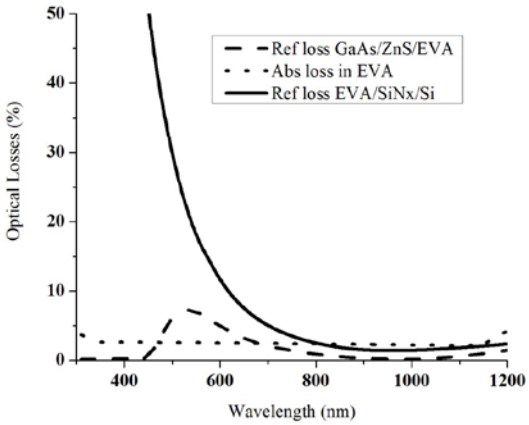


Figure 10, illustrates the light intensities available at the gallium arsenide and silicon surfaces and the various optical losses in the optimized tandem device architecture. The total front reflection and absorption losses before the light strikes the gallium arsenide surface is 119 W/m$^2$ or ~ 11.9% of the AM 1.5 spectral intensity. Light intensity incident on gallium arsenide surface, passing through gallium arsenide without absorption, optical loss at GaAs / Si interface, incident on silicon surface and light intensity incident on the back sheet are 881 W/m$^2$, 286.8 W/m$^2$, 13.6 W/m$^2$, 273.2 W/m$^2$ and 140 W/m$^2$ respectively.

Fig. 10

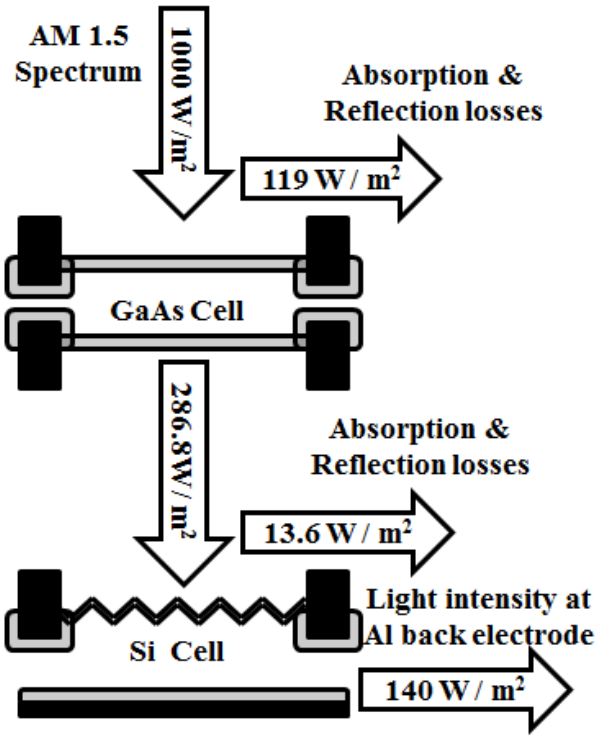


### 3.3. Electronic Simulation of the Gallium Arsenide and Silicon Devices:

Figure 11 shows the I-V curves of the simulated GaAs solar cell and the theoretical maximum (Shockley-Queisser limit) taking into account the optical losses in the device shown in figure 6. Electrical characteristics of the simulated gallium arsenide solar cell and the device fabricated at IMEC (Flamand et al., 2009) are shown in table 1. The difference in power conversion efficiencies between simulated and experimental devices is only 0.2%. The I-V characteristics of the simulated stand-alone silicon device was calculated by removing the gallium arsenide solar cell at the top and allowing the AM 1.5 spectrum to strike the silicon solar cell with silicon nitride antireflection coating and

EVA encapsulation layer. Comparing the stand alone silicon solar cell, tabulated in table 1, with the experimental device reported by Zhao et al. (1999), difference in power conversion efficiency was 2.1%. There is a slight over estimate in open circuit voltage and under estimate in short circuit current in the simulated gallium arsenide and stand alone silicon solar cells. This may be due to lower recombination rate of the simulated device and compared to the actual recombination rate leading to higher open circuit voltage and lower light absorption and reflection than estimated in anti-reflection coatings and encapsulation layer leading to lower short circuit current in the simulated device. Still the simulated gallium arsenide and stand alone silicon solar cells form a good fit with the experimental devices. The silicon tandem device was simulated with a modified light spectrum taking into account the light absorption and reflection at the top gallium arsenide solar cell and at the encapsulation above the silicon solar cell, the light intensity available at the silicon surface is 240 $W/m^2$. The I-V characteristics of the simulated and theoretical maximum Shockley - Queisser limit for tandem silicon solar cells are shown in figure 11. The power conversion efficiency of silicon tandem device was calculated to be 5.13% (referenced to the full AM 1.5 intensity) and the electrical characteristics are tabulated in table 1. Thus, the overall tandem structure can provide a combined efficiency of 28.5%, an impressive value. The increase in relative efficiency of GaAs / Si tandem solar cell, compared to standalone gallium arsenide solar cell efficiency is as high as 22%.

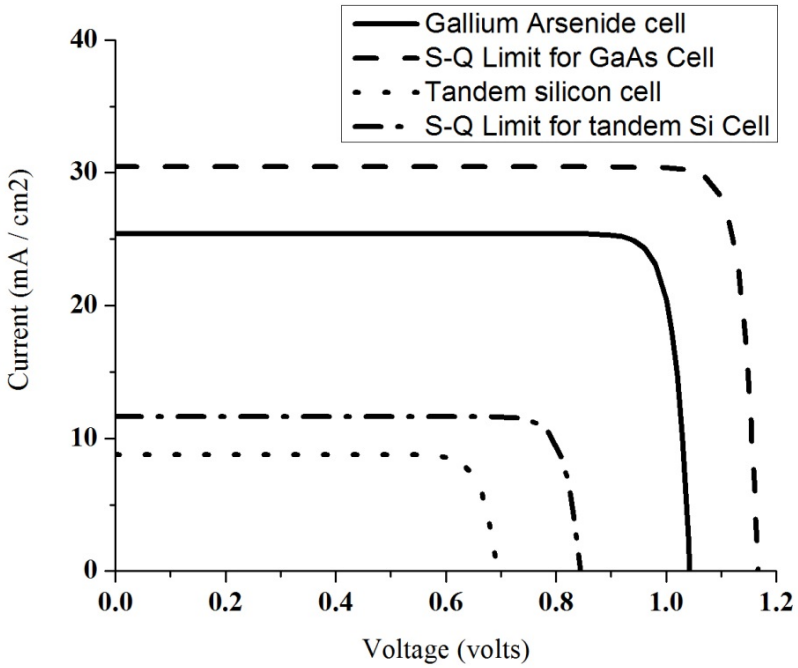


Fig. 11

Table 1. Current-voltage characteristics of the simulated and experimental devices.

| Simulated Data | Voc in mV | Jsc in mA/cm2 | FF in % | Efficiency in % |
|---|---|---|---|---|
| GaAs solar cell | 1042 | 25.42 | 88.4 | 23.4 |
| Stand alone silicon cell | 720 | 37 | 84.9 | 22.6 |
| Tandem silicon solar cell | 692 | 8.8 | 84.2 | 5.13 |
| Experimental cell efficiencies (from literature) | | | | |
| GaAs cell (Flamand et al., 2009) | 1037 | 27.7 | 80.8 | 23.2 |
| Stand alone silicon cell (Zhao et al. 1999) | 704 | 42 | 83.5 | 24.7 |

Voltage, current and power loss percentages of the gallium arsenide and tandem silicon solar cell were calculated by comparing the simulated device characteristics with Shockley-Queisser values and the calculated loss percentages are tabulated in table 2. The higher current, voltage loss and hence higher power loss for tandem silicon solar cells compared to gallium arsenide solar cell is due to lower back surface and bulk recombination rate in gallium arsenide solar cell compared to the silicon solar cell.

Table 2. Electrical loss in the devices.

| Device | 1 - (Voc simulated / Voc Shockley-Queisser) (Voltage loss in %) | 1 - (Jsc simulated / Jsc Shockley-Queisser) (Current loss in %) | 1 - (Pmax simulated / Pmax Shockley-Queisser) (Power loss in %) |
|---|---|---|---|
| GaAs cell | 10.1 | 16.4 | 26.4 |
| Tandem Si cell | 18 | 24.5 | 39.2 |

Figure 12 provides the quantum efficiencies of gallium arsenide and silicon solar cells used in the simulation. Gallium arsenide solar cell has lower quantum efficiency in UV to 500 nm wavelength because of the light absorption in the zinc sulfide antireflection and gallium indium phosphide window layers. Silicon because of its indirect band gap is known to have low absorption near its band edge as seen in figure 12. So a further improvement in efficiency of tandem silicon solar cell is possible by developing silicon solar cell architectures with improved infra-red light absorption properties. This would not only reduce the silicon consumption in the device and also increase the device efficiency. Figure 11 shows the Shockley-Queisser limit for tandem silicon cell with gallium arsenide solar cell, the maximum possible efficiency for the tandem silicon cell is calculated to be 8.35%.

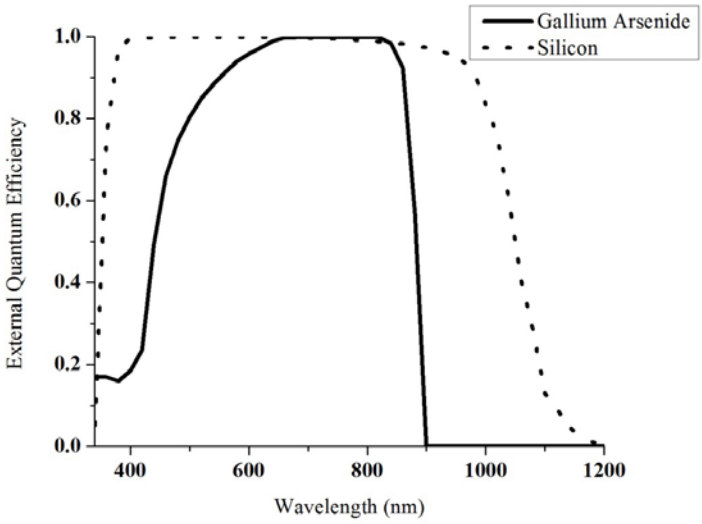


Fig. 12

**4. Conclusion & Future work:**

A detailed quantitative simulation model of a mechanical gallium arsenide / silicon tandem device was developed. Optical losses in the tandem device was studied for AM 1.5 solar spectrum considering the absorption and reflection losses at the antireflection coatings and encapsulation layers. Electrical performance of stand-alone and tandem devices was analyzed and it was noted that 28.5% efficient tandem devices could be made with present generation of devices. The improvement in efficiency is due to increased absorption at infrared wavelengths from 870 nm to 1200 nm. Further improvements in efficiency approaching 30% may be possible with more optimized nano-structured silicon surface features that are tuned to emphasize light scattering further into the relevant near infra-red spectral region (between 800 and 1200 nm). Tandem devices of more than 30% efficiencies are also possible using top cells with a band gap of 1.7 eV ~ 2.1 eV replacing the gallium arsenide device used in the present model and

conventional silicon solar cells could potentially be used at the bottom, as shown in figure 1. Efficient high band gap solar cell devices need to be researched and developed as potential strategies to improve device efficiencies beyond 30%.

**Acknowledgement:**

We would like to thank Mr. Moon Hee Kang of Georgia Tech for providing his experimental data on SiNx which is used in developing the simulation models. We would like to acknowledge Prof. Rockett, Dr. Yiming Liu of University of Illinois at Urbana Champaign and Prof. Fonash of Pennsylvania State University for developing and providing open access to WxAMPS simulation software. We appreciate support from the Corning/Saint-Gobain/Malcolm G. McLaren Endowment at Rutgers University.

**References:**

Aberle, A.G. 2000. Surface passivation of crystalline silicon solar cells: a review. Prog. in Photovolt.: Res and Appl. 8(5), 473–487. DOI: 10.1002/1099-159X(200009/10)8:5<473::AID-PIP337>3.0.CO;2-D.

Adachi, S. 1999. Optical Constants of Crystalline and Amorphous Semiconductors – Numerical Data and Graphical Illustration. Kluwer Academic Publishers, Massachusetts.

Bauhuis, G. J., Mulder, P., Haverkamp, E. J., Huijben, J. C. C. M., and Schermer, J. J. 2009. 26.1% thin-film GaAs solar cell using epitaxial lift-off. Sol. Energ. Mat. Sol. C. 93(9), 1488-1491. DOI: 10.1016/j.solmat.2009.03.027.

Belghachi, A., and Helmaoui, A. 2008. Effect of the front surface field on GaAs solar cell photocurrent. Sol. Energ. Mat. Sol. C. 92(6),667-672.DOI:10.1016/j.solmat.2008.02.003.

Bertness, K.A., Kurtz, S.R., Friedman, D.J., Kibbler, A.E., Kramer, C., and Olson, J.M. 1990. 29.5%-efficient GaInP/GaAs tandem solar cells. Appl. Phys. Lett. 65(8), 989. DOI:10.1063/1.112171.

Bozler, C. O., R. W. McClelland, and J. C. C. Fan. 1981. Ultrathin, high efficiency solar cells made from GaAs films prepared by the CLEFT Process. IEEE Electron Devic. Lett. 2 (8), 203-205. DOI: 10.1109/EDL.1981.25402.

Burgess, R.M., Stanbery, B.J., Mickelsen, R.A., Avery, J.E., McClelland, R.W., King, B.D., Boden, M.J., and Gale, R.P. 1988. High efficiency GaAs / CuInSe2 tandem junction solar cells. 20th IEEE Photovolt. Specialists Conf. 1, 457 - 461. DOI: 10.1109/PVSC.1988.105743.

Chen, A., and Zhu, K. 2012. Computer simulation of a-Si/c-Si heterojunction solar cell with high conversion efficiency. Sol. Energy 86(1), 393-397. DOI: 10.1016/j.solener.2011.10.015.

Dao, V.A., Heo, J., Choi, H., Kim, Y., Park, S., Jung, S., Lakshminarayan, N., and Yi, J. 2010. Simulation and study of the influence of the buffer intrinsic layer, back-surface field, densities of interface defects, resistivity of p-type silicon substrate and transparent conductive oxide on heterojunction with intrinsic thin-layer (HIT) solar cell. Sol. Energy 84(5), 777-783. DOI: 10.1016/j.solener.2010.01.029.

Dwivedi, N., Kumar, S., Bisht, A., Patel, K., and Sudhakar, S. 2013. Simulation approach for optimization of device structure and thickness of HIT solar cells to achieve ~ 27% efficiency. Sol. Energy 88, 31-41. DOI: 10.1016/j.solener.2012.11.008.

Fellmeth, T., Mack, S., Bartsch, J., Erath, D., Jäger, U., Preu, R., Clement, F., and Biro, D. 2011. 20.1% Efficient Silicon Solar Cell With Aluminum Back Surface Field. IEEE Electron Device Lett., 32(8), 1101 - 1103. DOI: 10.1109/LED.2011.2157656.

Flamand, G., Zhao, L., Mols, Y., Van der Heide, J., and Poortmans, J. 2009. Development of Mechanically Stacked Multi-Junction Solar Cells Applying Thin, One-side Contacted III-V Cells. 24th European Photovolt. Sol. Energy Conf. 126-129. DOI: 10.4229/24thEUPVSEC2009-1BO.5.5.

French, R.H., Rodriguez-Parada, J.M., Yang, M.K., Derryberry, R.A., Lemon, M.F., Brown, M.J., Haeger, C.R., Samuels, S.L., Romano, E.C., and Richardson, R.E. 2009. Optical properties of materials for concentrator photovoltaic systems. 34th IEEE Photovolt. Specialists Conf. 000394-000399. DOI: 10.1109/PVSC.2009.5411657.

Gale, R.P., McClelland, R.W., Dingle, B.D., Gormley, J.V., and Burgess, R.M. 1990. High efficiency GaAs / CuInSe2 and AlGaAs / CuInSe2 thin-film tandem solar cells. 21st IEEE Photovolt. Specialists Conf. 1, 53-57. DOI: 10.1109/PVSC.1990.111590.

Gee, J. M., and Virshup, G. F. 1988. A 31% efficient GaAs / silicon mechanically stacked, multijunction concentrator solar cell. 20th IEEE Photovolt. Specialists Conf. 1, 00754-00758. DOI: 10.1109/PVSC.1988.105803.

Griggs, M. J., Kayes, B. M. and Atwater, H. A. 2006. pn junction heterostructure device physics model of a four junction solar cell. Proc. of the SPIE, 6339, 63390D. DOI: 10.1117/12.680793.

Henry, C.H. 1980. Limiting efficiencies of ideal single and multiple energy gap terrestrial solar cells. J. Appl. Phys. 51(8), pp. 4494 - 4500. DOI: 10.1063/1.328272.

Ito, S., Dharmadasa, I. M., Tolan, G. J., Roberts, J. S., Hill, G., Miura, H.,Yum, J-H, Pechy, P., Liska, P., Comte, P., and Grätzel, M. 2011. High-voltage (1.8 V) tandem solar cell system using a GaAs/AlXGa (1-X)As graded solar cell and dye-sensitised solar cells with organic dyes having different absorption spectra. Sol. Energy 85(6), 1220-1225. DOI: 10.1016/j.solener.2011.02.024.

Kang, M.H., Ryu, K.R., Upadhyaya, A., Rohatgi, A. 2011. Optimization of SiN AR coating for Si solar cells and modules through quantitative assessment of optical and efficiency loss mechanism. Prog. in Photovolt.: Res. and Appl. 19(8), 983–990. DOI: 10.1002/pip.1095.

Karam, N.H., King, R., Cavicchi, T.B.,, Krut, D.B., Ermer, J.H., Haddad, M., Cai, L., Joslin, D.E., Takahashi, M., Eldredge, J.W., Nishikawa, W.T., Lillington, D.T., Keyes, B.M., and Ahrenkiel, R.K. 1999. Development and Characterization of High Efficiency Ga0.5In0.5P / GaAs / Ge Dual- and Triple-Junction Solar Cells. IEEE Trans. on Electron Devic. 46(10), 2116 - 2125. DOI: 10.1109/16.792006.

King, R.R., Law, D.C., Edmondson, K.M., Fetzer, C.M., Kinsey, G.S., Yoon, H., Sherif, R.A., and Karam, N.H. 2007. 40% efficient metamorphic GaInP / GaInAs / Ge multijunction solar cells. Appl. Phys. Lett. 90(18), 183516. DOI:10.1063/1.2734507.

Lee, K., Zimmerman, J. D., Zhang, Y. and Forrest, S. R. 2012. Epitaxial lift-off of GaAs thin-film solar cells followed by substrate reuse. 38th IEEE Photovolt. Specialists Conf. 001698-001700. DOI: 10.1109/PVSC.2012.6317922.

Lin, L. J., and Chiou, Y. P. 2012. Improving thin-film crystalline silicon solar cell efficiency with back surface field layer and blaze diffractive grating. Sol. Energy, 86(5), 1485-1490. DOI: 10.1016/j.solener.2012.02.009.

Liska, P., Thampi, K.R., Grätzel, M., Brémaud, D., Rudmann, D., Upadhyaya, H.M., and Tiwari, A.N. 2006. Nanocrystalline dye-sensitized solar cell / copper indium gallium selenide thin-film tandem showing greater than 15% conversion efficiency. Appl. Phys. Lett. 88(20), 203103. DOI: 10.1063/1.2203965.

Liu, Y., Sun, Y., and Rockett, A. 2012. A new simulation software of solar cells—WxAMPS. Sol. Energ. Mater. Sol. C. 98, 124-128. DOI:10.1016/j.solmat.2011.10.010.

Mattos, L. S., Scully, S. R., Syfu, M., Olson, E., Yang, L., Ling, C., Kayes, B.M. and He, G. 2012. New module efficiency record: 23.5% under 1-sun illumination using thin-film single-junction GaAs solar cells. 38th IEEE Photovolt. Specialists Conf. 003187-003190. DOI: 10.1109/PVSC.2012.6318255.

Mehta, S., 2012. PV Technology, Production and Cost Outlook: 2012-2016. Green Tech Media Research. <http://www.greentechmedia.com/research/report/pv-supply-2012>.

Papet, P., Nichiporuk, O., Kaminski, A., Rozier, Y., Kraiem, J., Lelievre, J.F., Chaumartin, A., Fave, A., Lemiti, M. 2006. Pyramidal texturing of silicon solar cell with TMAH chemical anisotropic etching. Sol. Energ. Mater. Sol. C. 90(15), 2319-2328. DOI: 10.1016/j.solmat.2006.03.005.

Plá, J., Barrera, M., and Rubinelli, F. 2007. The influence of the InGaP window layer on the optical and electrical performance of GaAs solar cells. Semicond. Sci. Tech. 22(10), 1122-1130. DOI: 10.1088/0268-1242/22/10/008.

Shockley, W., and Queisser, H.J. 1961. Detailed Balance Limit of Efficiency of pn Junction Solar Cells. J. of Appl. Phys., 32(5), 510-519. DOI: 10.1063/1.1736034.

Siqueiros, J. M., Machorro, R., and Regalado, L. E. 1988. Determination of the optical constants of MgF2 and ZnS from spectrophotometric measurements and the classical oscillator method. Appl. Optics. 27(12), 2549-2553. DOI: 10.1364/AO.27.002549.

US Energy Information Administration, 2011. International Energy Outlook 2011. <http://www.eia.gov/forecasts/ieo/pdf/0484(2011).pdf>

Woodhouse, M., James, T., Margolis, R., Feldman, D., Merkel, T., and Goodrich, A. 2011. An Economic Analysis of Photovoltaics Versus Traditional Energy Sources: Where Are We Now and Where Might We Be in the Near Future? 37th IEEE Photovolt. Specialists Conf. (PVSC 37) 2481 - 2483.

Zhao, J., Wang, A., and Green, M.A. 1999. 24.5% Efficiency silicon PERT cells on MCZ substrates and 24.7% efficiency PERL cells on FZ substrates. Prog. in Photovolt. Res. and Appl. 7(6), 471 - 474. DOI: 10.1002/(SICI)1099-159X(199911/12)7:6<471::AID-PIP298>3.0.CO;2-7.

Zhao, L., Zhou, C.L., Li, H.L., Diao, H.W., and Wang, W.J. 2008. Design optimization of bifacial HIT solar cells on p-type silicon substrates by simulation. Sol. Energ. Mat. Sol. C. 92(6), 673-681. DOI: 10.1016/j.solmat.2008.01.018.

Zhao, L., Li, H. L., Zhou, C. L., Diao, H. W., and Wang, W. J. 2009. Optimized resistivity of p-type Si substrate for HIT solar cell with Al back surface field by computer simulation. Sol. Energy 83(6), 812-816. DOI: 10.1016/j.solener.2008.11.007.

**Figure Captions:**

1. a) Theoretical conversion efficiencies based on Shockley and Queisser limit and b) two junction (mechanical stack) solar cells under AM 1.5 solar spectrum.
2. Illustration of the proposed GaAs/Si tandem solar cell.
3. Illustration of the modeled gallium arsenide solar cell.
4. Illustration of the modeled silicon solar cell.

5. Extinction Coefficient of the materials used in the tandem device.
6. Refractive Index of the materials used in the tandem device.
7. Optical loss due to various layers in the top cell before the light gets absorbed by the gallium arsenide layer.
8. Light spectrum incident on the tandem device, absorbed by gallium arsenide cell and silicon cell.
9. Optical loss due to various layers in the bottom cell before the light gets absorbed by the silicon layer.
10. Illustration of the light intensity available at gallium arsenide and silicon surfaces and the various optical losses in the device.
11. Simulated and theoretical maximum current-voltage curves for silicon solar cell in tandem with gallium arsenide solar cell.
12. External Quantum Efficiency of simulated gallium arsenide and silicon solar cells.

**Table Captions:**

Table 1. Current-voltage characteristics of the simulated and experimental devices.

Table 2. Electrical loss in the devices.